Effect of Reduced RF Gradient on MICE Cooling Performance

C.T. Rogers

Abstract

In MICE, we hope to operate two four-cavity linacs that will replace energy lost by muons in the absorbing medium. In the MICE design, these cavities will be bathed in an intense solenoidal field that provides transverse focussing. Recent (and not-so-recent) experiments have indicated that there may be some risk that the superposition of magnetic fields reduces the peak achievable RF gradient in the cavities. This may reduce the RF gradient available for MICE, and hence the energy recovered by the MICE beam. In this note I explore the impact this may have on the MICE experiment.

EVIDENCE FOR REDUCED RF VOLTAGE IN MAGNETIC FIELDS

Four RF cavities have been operated in the MUCOOL Test Area (MTA) at Fermilab. The cavities were operated in conjunction with the so-called Lab-G solenoid, a two coil solenoid capable of generating fields up to 4 T with the coils operating with the same polarity or fields of 0.7 T with a gradient of 20 T/m with the coils operating at opposite polarity in bucking mode.

A 4-cavity 805 MHz open-cell structure sealed at each end by Titanium vacuum windows was operated in solenoidal fields up to 4 T [1]. No reduction in peak RF field was observed when the solenoid was running, but radiation levels were 4 times higher on axis and evidence of physical damage to the windows was observed, to the extent that the vacuum seal was broken.

A single 805 MHz cavity was operated with button inserts to enable testing of different materials and coatings [2] in fields up to 4 T. In these tests, a strong dependence of peak achievable gradient on magnetic field was observed. Operation in bucking mode showed the same dependence of peak RF gradient on magnetic field. However, later examination of the cavity revealed evidence of breakdown in the RF coupler, indicating that the RF coupler may have limited the gradient that could be achieved.

A single 201 MHz cavity [3] was tested in the fringe field of the Lab-G magnet. Initial results indicate a dependence on the magnetic field, but testing has been frustated by a lack of RF power at 201 MHz and the cost of a large aperture solenoid that can contain the higher radius RF cavity.

A single 805 MHz cavity fitted to contain a high pressure gas was operated with a variety of button inserts [4]. The cavity was not operated in high vacuum, but operation at pressures between air pressure and 1300 psi showed no dependence of the peak achievable gradient on magnetic field.

Two models have been proposed to predict a dependence on RF voltage in magnetic fields. In the Twist model [2], a strong electric current flows at the tip of an asperity where the RF field is enhanced. This creates a torsional force that tears the tip of asperity from the surface causing damage that leads to further asperities. In the field-emission focussing model [3], electrons emitted by asperities are focussed by the magnetic field on to the far side of the cavity, leading to heating, metal fatigue and the creation of further asperities.

The evidence for reduced RF voltage in magnetic fields is far from conclusive. In general for RF cavities the peak field gradient that can be achieved varies significantly between apparently identical cavities, but only one cavity of each type has been studied here. Even parameters such as the length of the RF pulse can play a significant role in determining the peak achievable gradient [5].

ARRANGEMENT IN MICE

If the peak achievable RF gradient is lower than expected, MICE will not be able to demonstrate energy recovery, a key part of the ionisation cooling channel. In addition, it will not be possible to assess the impact of high RF gradients on the MICE hardware. For example, we will not be able to study effects that may be present, but are not expected, such as radiation damage to the liquid absorber windows. In this note I limit my study to the effect of the absence of RF cavities on the optics of the MICE lattice and the impact this has on the normalised emittance reduction in the cooling cell.

In the MICE baseline, the RF cavities will be operated at about 8 MV/m and on-crest (90° phase), such that all the energy lost in the absorber is replaced. This provides energy recovery, but in a long cooling channel, debunching would occur leading to significant longitudinal emittance growth. In the Neutrino Factory Feasibility Study 2 cooling section, upon which the MICE channel is based, the RF cavities are intended to operate at 15 MV/m and 40° phase [6]. MICE cannot afford sufficient RF power supplies to operate at this peak field gradient in Step 6. It has been suggested that MICE operate in a bunching mode in Step 5, using the power supplies that will eventually be available for Step 6 to provide the additional gradient. The practicalities and cost of bringing extra waveguides around the MICE hall may make this impossible.

Additional modes have been proposed, where MICE operates with the coupling coil in opposite polarity to the focus coils, such that the magnetic field changes direction across the RF cavities. This may reduce the effect of magnetic field on the cavities, although there is some empirical

evidence to indicate that this is not the case.

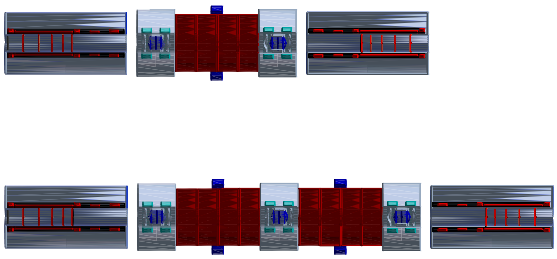

Figure 1: The geometry as simulated in G4MICE code (top) for MICE Step 5 and (bottom) for MICE Step 6. Absorbers and RF cavities are simulated with curved windows, while a field map generated by superfish [7] is used to model the RF cavities.

In this note I study MICE Step 5 and Step 6 for three cases: a pessimistic case where no RF is available; the baseline case with the nominal RF gradient available, 8.7 MV/m at 90° phase; and an optimistic case where 18 MV/m are available with MICE running at 30° degrees phase, which is close to the Study 2 baseline and indicative of the cooling channel that MICE is intended to prototype. The simulated geometry for MICE Step 5 and Step 6 is shown in Figure 1. By way of pessimism, even in the absence of accelerating voltage, the RF cavities were left in situ, leading to a larger emittance increase. If the RF cavity voltage is limited it is hoped that they would still provide some accelerating voltage; however, as I shall demonstrate MICE's cooling performance is unchanged even when there is no accelerating field at all.

I assume an arbitrary choice of initial beam conditions in this study and beams are generated from a multivariate gaussian distribution. In practice, the muons will have no time distribution on entering MICE and we will be able to select muons with an appropriate distribution. Significant position-energy correlations are expected to exist in the input muon beam and the energy spread may be rather large; I have assumed that an appropriate selection algorithm will be used to remove these correlations. Such a technique has been demonstrated for Monte Carlo 'truth' data [8] [9].

MICE STEP 5

Initially I simulate Step 5 of MICE, where only a half-cell of the cooling channel is present. Simulated particles sit at -3.225 m from the channel centre and they are subsequently tracked to +3.225 m from the channel centre. These positions correspond to the nominal position of the tracker measurement planes. The magnets are simulated with fields in flip mode for reference muon momentum of 200 MeV/c. The magnet geometry and currents is described in Table 1. Cavities are phased for a 200 MeV/c muon moving on axis, experiencing mean energy loss in absorbers and appropriate energy recovery in the RF cavities.

In all cases, a beam was generated with canonical transverse β=333 mm, α=0 and 6 mm emittance. For the 0 MV/m and 8.7 MV/m cases, there is no longitudinal focussing. In this case a slightly larger time spread is used and a smaller energy spread, while keeping longitudinal emittance constant, in order to reduce the non-linear effects of the muon energy on time-of-flight and so to keep the longitudinal emittance reasonably well controlled. For the 18 MV/m case, the RF provides focussing so that a periodic longitudinal phase space can be formed, and a larger energy spread is used with a smaller time spread. Additionally, a third moment correlation was added that correlates the energy with transverse amplitude, to more closely mimic a realistic Neutrino Factory beam and to reduce non-linear effects.

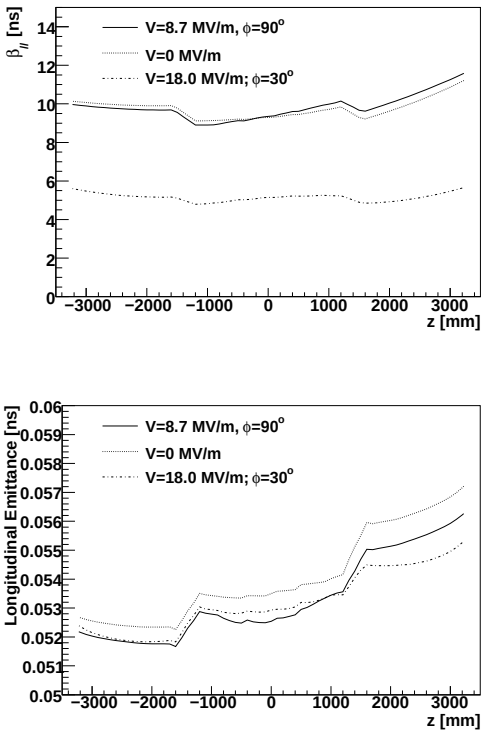

Figure 2: Evolution of (top) longitudinal β and (bottom) longitudinal emittance along MICE Step 5, after rejection of particles that fall outside of a fiducial cut of 150 mm radius and a longitudinal cut of 0.3 ns amplitude at either tracker reference plane.

The longitudinal β function and emittance is shown in Figure 2; here I assume that particles with longitudinal amplitude greater than 0.3 ns are outside of the transmission of the cooling channel and particles with radius greater than 150 mm are outside of the fiducial volume of the tracker. All cases show some longitudinal emittance growth. The principal contribution arises from energy straggling in the

Coil	Z1	Z2 Z1	R1	R2-R1	Zmean	Rmean	200 MeV/c
	MICE Step 5						
CC	-0.1250	0.2500	0.7250	0.1160	0.0000	0.7830	-96.21
FC2	1.0650	0.2100	0.2630	0.0840	1.1700	0.3050	-113.95
FC3	1.4750	0.2100	0.2630	0.0840	1.5800	0.3050	113.95
M1	2.1354	0.2012	0.2580	0.0447	2.2360	0.2804	118.56
M2	2.5763	0.1995	0.2580	0.0298	2.6761	0.2729	137.13
E1	3.0207	0.1106	0.2580	0.0596	3.0760	0.2878	127.37
C	3.1689	1.3143	0.2580	0.0213	3.8261	0.2687	152.44
E2	4.5207	0.1106	0.2580	0.0660	4.5760	0.2910	135.18
	MICE Step 6						
FC1	0.1	0.21	0.263	0.084	0.2050	0.3050	-113.95
CC	1.25	0.25	0.725	0.116	1.3750	0.7830	-96.21
FC2	2.44	0.21	0.263	0.084	2.5450	0.3050	-113.95
FC3	2.85	0.21	0.263	0.084	2.9550	0.3050	113.95
M1	3.5104	0.2012	0.258	0.0447	3.6110	0.2804	118.56
M2	3.9513	0.1995	0.258	0.0298	4.0511	0.2729	137.13
E1	4.3957	0.1106	0.258	0.0596	4.4510	0.2878	127.37
C	4.5439	1.3143	0.258	0.0213	5.2011	0.2687	152.44
E2	5.8957	0.1106	0.258	0.066	5.9510	0.2910	135.18

Table 1: Geometry of the magnet elements in MICE Step 5 and 6. The geometry is reflected about $z = 0$. In Step 6 only, current polarities are reversed for coils with $z < 0$. Units are m and A/mm^2.

absorber and RF cavity windows, although there is some optical heating.

The longitudinal phase space at the downstream end of Step 5 is shown in Figure 3. For the baseline case, low energy muons arrive late giving rise to a long tail. Higher energy particles have velocities approaching the speed of light, and so the high energy tail is less pronounced; a particle travelling at the speed of light would take about 21.5 ns to traverse the channel. This effect is enhanced by the operation of RF on-crest, as late particles arrive off-crest, receive a smaller energy boost or even an energy reduction and arrive even later at the tracker, resulting in a more pronounced low energy tail. Meanwhile earlier particles also arrive off-crest, receive a smaller energy boost and so tend to stay relatively closer to the main body of the bunch, resulting in a very blunt high energy tail. In a longer system, these effects would give rise to significant emittance growth, but in the few metres of the MICE channel the nonlinear effects are not catastrophic. When the RF is applied at 30°, the bunch generally stays much more well defined. There is still a low energy tail, in this case due to particles which initially sit outside the RF bucket, but excepting this set of particles the muons are generally well behaved.

The transverse β function, transverse emittance and 6D emittance is shown in Figure 4. MICE has been designed assuming that the effects of energy loss on the transverse optics is negligible. This is a good approximation where energy is recovered in RF cavities. While the evolution of the transverse β function is effected slightly by the rather different energy loss, the effects on the evolution of emittance are negligible. In all cases the total 6d emittance reduction is of order 2-3 $\%$, averaged over each dimension; this is probably measurable by the MICE detector system, but would be a rather marginal result.

MICE STEP 6

I go on to simulate Step 6 of MICE, where a full cell of the cooling channel is present. In this case, particles are tracked from z=-4.6 m to z=+4.6m. These positions correspond to the nominal position of the tracker measurement planes. Magnets are simulated with fields in flip mode for the reference muon momentum of 200 MeV/c. The magnet geometry and currents is described in Table 1. The beam was set-up as in Step 5.

The features exhibited by MICE Step 5 can also be seen for Step 6, but results are more pronounced. The longitudinal β evolves normally but longitudinal emittance growth is considerable, especially for the case where no RF at all is present. Note that the initial longitudinal emittance of the beam input into MICE is lower for the 0 MV/m case. This is because particles with large longitudinal amplitude experience considerable emittance growth and are considered lost from the channel by the longitudinal amplitude cut criterion.

The longitudinal phase space at the downstream end of Step 6 looks similar to that of Step 5 but with stronger debunching effects. The case with 18 MV/m RF shows a noticeably more tightly bunched beam, with a tail of particles that were not initially in the RF bucket. This tail is more pronounced in the cases where no RF is present.

A noticeable mismatch is introduced into the transverse

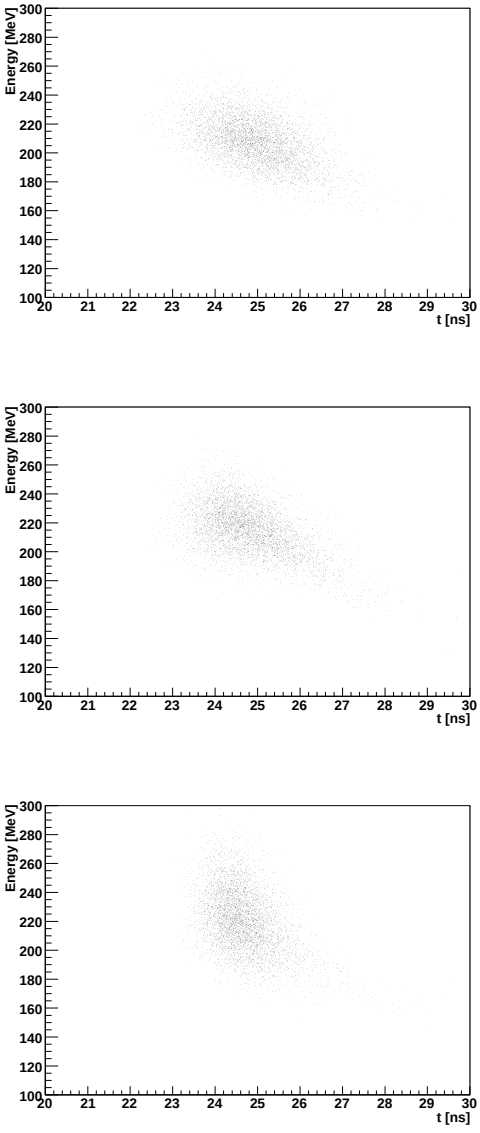

Figure 3: Energy-time phase space of the muon beam at the end of the Step 5 for (top) 0 MV/m (middle) 8.7 MV/m (bottom) 18 MV/m.

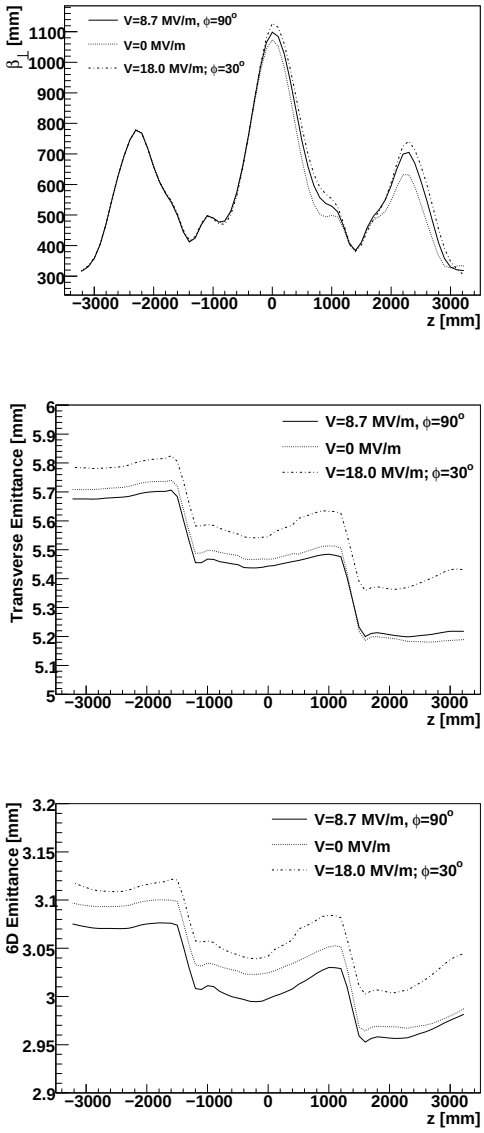

Figure 4: Evolution of (top) transverse β (middle) transverse emittance and (bottom) 6d emittance along MICE Step 5, after rejection of particles that fall outside of a fiducial cut of 150 mm radius and a longitudinal cut of 0.3 ns amplitude at either tracker reference plane.

phase space for the 0 MV/m case by the end of the cooling section, but this does not seem to have a strong effect on the cooling performance. The larger energy spread of the beam for the 18 MV/m case leads to quite large transverse heating, and so the transverse emittance reduction is smaller. Overall all 3 cases lead to a reduction of about 4 % in 6D emittance, averaged over each dimension (10-15 % for all 3 dimensions combined).

It seems that the emittance reduction is fairly insensitive to the presence, or lack thereof, of RF cavities. In the Neutrino Factory studies, it has been found to be useful to examine the change in the number of muons falling within some acceptance. In Figure 8 the fractional change in the number of muons within a transverse and longitudinal amplitude cut is plotted. Here the number of muons within the cut is calculated with some attempt to remove the effect of tails that might otherwise skew the distribution. It is clear that the increase is mostly independent of the longitudinal amplitude, but rather strongly dependent on the transverse amplitude, where particles in the fringe of the distribution tend to be lost more easily. The increase is independent of the presence of RF cavities.

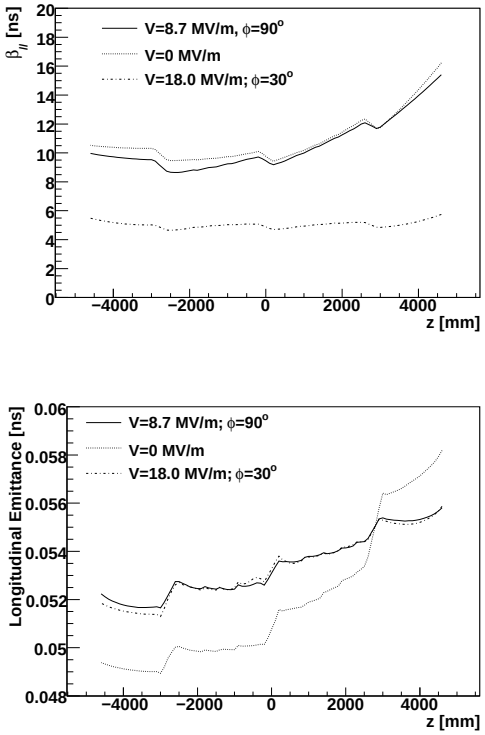

Figure 5: Evolution of (top) longitudinal β and (bottom) longitudinal emittance along MICE Step 6, after rejection of particles that fall outside of a fiducial cut of 150 mm radius and a longitudinal cut of 0.3 ns amplitude at either tracker reference plane.

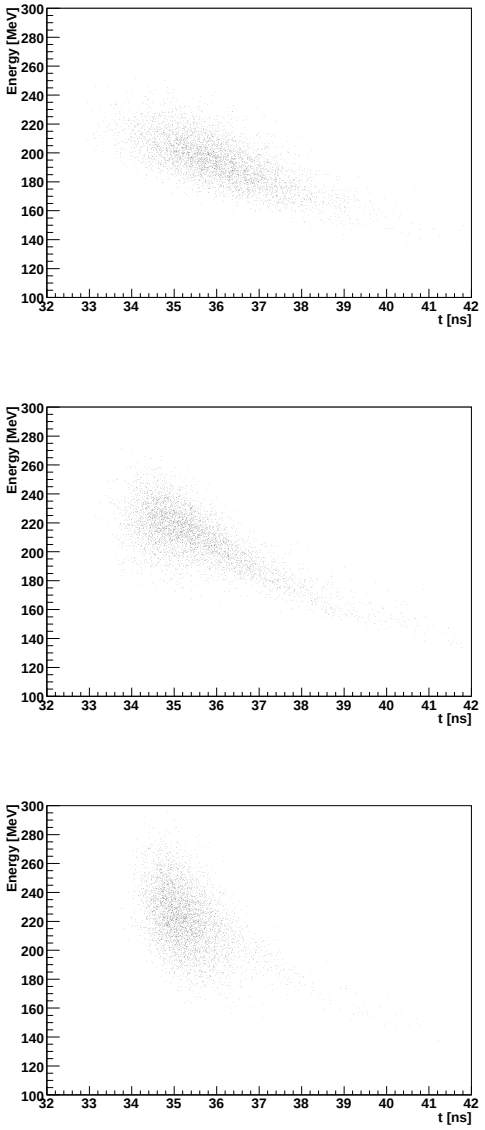

Figure 6: Energy-time phase space of the muon beam at the end of the Step 6 for (top) 0 MV/m (middle) 8.7 MV/m (bottom) 18 MV/m.

CONCLUSION

The peak voltage that may be achieved in the MICE cavities is unknown, but the community has a strong suspicion that it may be considerably reduced. If the MICE cavities do not operate with the nominal gradient, it will compromise the test of the engineering viability of a muon ionisation cooling channel. However, the reduction of 6D emittance seems to be reasonably independent of the presence, or not, of RF cavities.

REFERENCES

[1] J. Norem et al, Dark Current, Breakdown and Magnetic Effects in a Multicell, 805 MHz Cavity, PRSTAB 6, 072001, 2003.

[2] A. Moretti et al, Effects of High Solenoidal Magnetic Fields on RF Accelerating Cavities, PRSTAB 8, 072001, 2005.

[3] R.B. Palmer ,R.C. Fernow, J.C. Gallardo, D. Stratakis, RF Breakdown with External Magnetic Fields in 201 and 805 MHz Cavities, PRSTAB 12, 031002, 2009.

[4] M. Bastaninejad et al, Studies of Breakdown in a High Pressurised RF Cavity, Proc. EPAC 2008.

[5] V.A. Dolgashev et al, High-Power Tests of Normal Conducting Single-Cell Structures, Proc. PAC 2007.

[6] Ed. S. Ozaki, R. Palmer, M. Zisman, and J. Gallardo, Feasibility Study-II of a Muon-Based Neutrino Source, BNL-52623, 2001.

[7] K. Halbach and R. F. Holsinger, SuperFish - A Computer Program for Evaluation of RF Cavities with Cylindrical Symmetry, Particle Accelerators 7, 213-222, 1976.

[8] C.T. Rogers, Statistical weighting of the MICE Beam, Proceedings of the 11th European Particle Accelerator Conference, 2008.

[9] C.T. Rogers and P. Snopok, Wedge Absorber Simulations for the Muon Ionisation Cooling Experiment, Proceedings of COOL 2009.

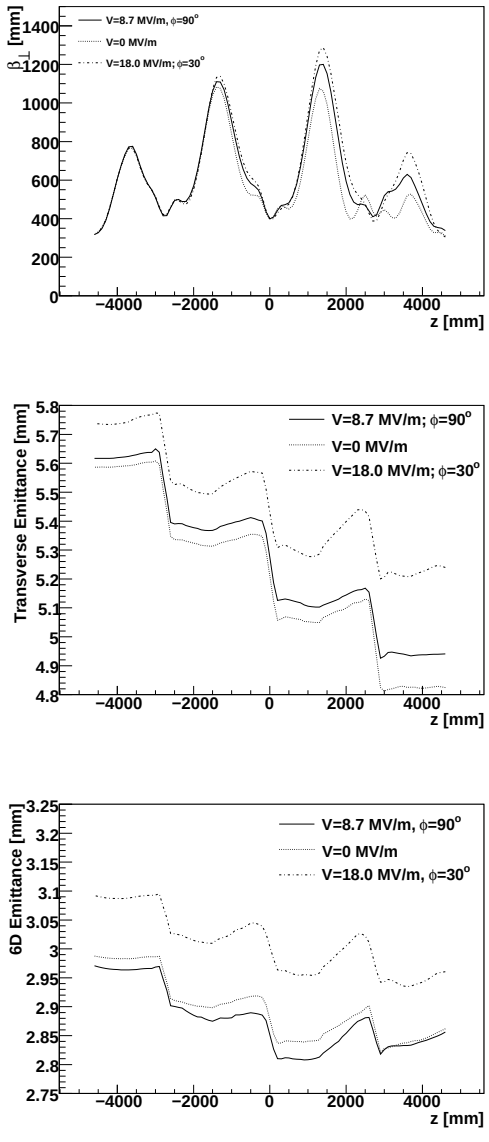

Figure 7: Evolution of (top) transverse β (middle) transverse emittance and (bottom) 6d emittance along MICE Step 6, after rejection of particles that fall outside of a fiducial cut of 150 mm radius and a longitudinal cut of 0.3 ns amplitude at either tracker reference plane.

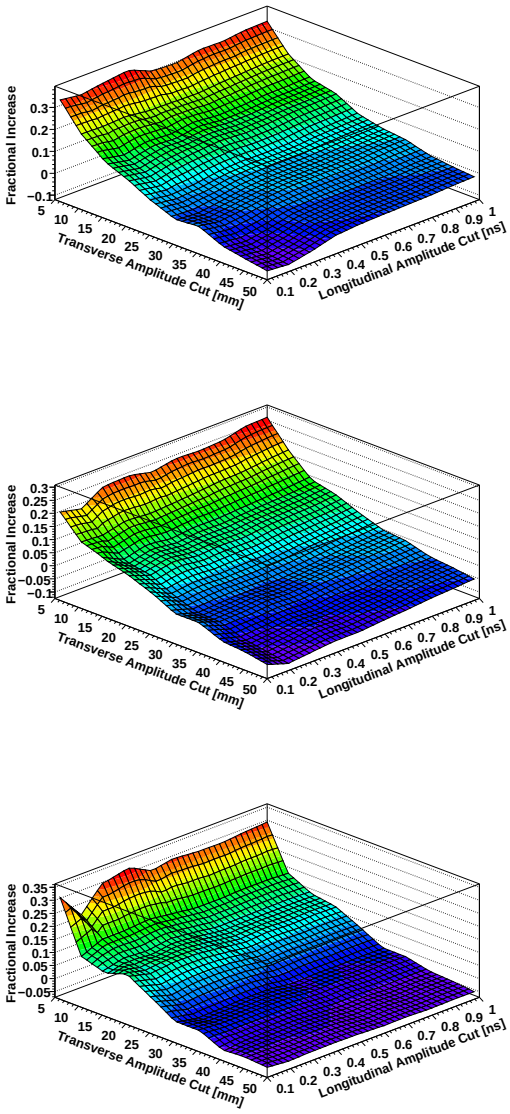

Figure 8: Fractional increase in number of muons within a transverse and longitudinal amplitude cut for RF voltage and phase of (top) 0 MV/m (middle) 8.7 MV/m, 90° phase and (bottom) 18 MV/m and 30° phase, in Step 6.